Reprinted From
From Nuclei to Particles
© 1981, LXXIX Corso
Soc. Italiana di Fisica - Bologna - Italy

13

The Shell Model Potential from a Relativistic Hartree-Fock Approach.

M. JAMINON, C. MAHAUX and P. ROCHUS

Institute de Physique, Université de Liège - Liège, Belgium

1. – Introduction.

WALECKA [1] and collaborators [2, 3] have recently developed a model relativistic quantum field theory of nuclear matter and of finite nuclei. In the simplest and most investigated form of this model, the nucleon field interacts with a neutral scalar-meson (σ) field and with a neutral vector-meson (ω) field. Although this is a daring over-simplification of the nuclear Lagrangian, the model deserves detailed scrutiny not only because it yields fair agreement with a number of experimental data, but mainly because it includes some mesonic degrees of freedom in a way which is completely consistent with the requirements of relativistic quantum field theory. All equations, therefore, appear in a Lorentz-covariant form. In particular, it is natural that in this approach the single-particle wave equation of the shell model emerges in the form of the relativistic Dirac equation rather than in the form of the nonrelativistic Schrödinger equation. The present paper is mainly devoted to this relativistic single-particle wave equation and to its relationship with the familiar nonrelativistic shell model potential. More specifically, our main purpose is twofold: i) We discuss the relativistic Hartree-Fock approximation. While the Hartree approximation has already been investigated in some detail in the available literature [4-7], the Fock contribution had never been properly investigated. ii) We construct a local single-particle potential which can be introduced in the Schrödinger equation and then yields exactly the same phase shift and bound-state energies as those which would be obtained from the relativistic wave equation. This step is largely independent of the (*e.g.* Hartree or Hartree-Fock) approximation which has led to a relativistic wave equation, whence its intrinsic interest.

The main features of the relativistic quantum field model are briefly described in sect. 2. The Hartree and the Hartree-Fock approximations are investigated in sect. 3 and 4, respectively. In sect. 5, we discuss some limitations and possible extensions of our work. In many instances we write the equations only in the limit of infinite nuclear matter, in which they take a simpler and more transparent form.

2. – The relativistic quantum field model.

Following WALECKA [1] and others [4, 5], we adopt the following Lagrangian density:

$$\mathscr{L} = \mathscr{L}^{\text{free}}_{\mathscr{N}} + \mathscr{L}^{\text{free}}_{\sigma} + \mathscr{L}^{\text{free}}_{\omega} + \mathscr{L}^{\text{int}}_{\sigma\mathscr{N}} + \mathscr{L}^{\text{int}}_{\omega\mathscr{N}}, \tag{1}$$

where the last two terms, respectively, describe the interaction between the nucleon $\mathscr{N}$, on the one hand, and the scalar meson σ and the vector meson ω, on the other hand. The relativistic single-particle potential can be identified with the self-energy operator. The most systematic calculational procedure probably consists in expanding the self-energy in powers of the strength of the meson-nucleon interaction [8]. Alternative methods exist, see, *e.g.*, ref. [1, 9]. These methods are largely equivalent in the Hartree approximation. Here it is convenient to adopt the presentation of Miller and Green [4] and of Brockmann [5], to whom we refer for further detail. These authors treat the meson fields as classical fields; this implies the omission of all quantities containing annihilation or creation operators for antiparticles and renders this approach inappropriate for going beyond the Hartree-Fock approximation in a systematic way. They obtain the following nuclear Hamiltonian:

$$\begin{aligned} H = &\sum_{\alpha,\alpha'} \int d^3x\, f^\dagger_{\alpha'}(\boldsymbol{x})\gamma_0(-i\boldsymbol{\gamma}\cdot\boldsymbol{\nabla} + m) f_\alpha(\boldsymbol{x})\, b^\dagger_{\alpha'} b_\alpha + \\ &+ \tfrac{1}{2} \sum_{\substack{\alpha,\alpha' \\ \delta,\delta'}} \int d^3x_1 d^3x_2\, f^\dagger_{\alpha'}(\boldsymbol{x}_1) f^\dagger_{\delta'}(\boldsymbol{x}_2)\, V^{\alpha\alpha'}(|\boldsymbol{x}_1 - \boldsymbol{x}_2|) f_\delta(\boldsymbol{x}_2) f_\alpha(\boldsymbol{x}_1) b^\dagger_{\alpha'} b^\dagger_{\delta'} b_\delta b_\alpha . \end{aligned} \tag{2}$$

Here $\{f_\alpha(\boldsymbol{x})\}$ is a complete set of Dirac spinors and b_α (respectively, $b^\dagger_\alpha$) denotes an annihilation (respectively, a creation) operator for a nucleon in state α. The nucleon-nucleon interaction in eq. (2) reads

$$V^{\alpha\alpha'}(|\boldsymbol{x}_1 - \boldsymbol{x}_2|) = \sum_{i=\sigma,\omega} \Gamma_i(1, 2)\, V_i^{\alpha\alpha'}(|\boldsymbol{x}_1 - \boldsymbol{x}_2|) \tag{3}$$

with

$$\Gamma_\sigma(1, 2) = -\gamma_0(1)\gamma^0(2), \tag{4}$$

$$\Gamma_\omega(1, 2) = \gamma_0(1)\gamma^0(2)\gamma_\mu(1)\gamma^\mu(2), \tag{5}$$

$$\begin{aligned} V_i^{\alpha\alpha'}(r) = \frac{g_i^2}{4\pi} \frac{\Lambda_i^2}{\Lambda_i^2 - m_i^2} \frac{1}{r} \{ &\exp[-r[m_i^2 - (E_\alpha - E_{\alpha'})^2]] - \\ &- \exp[-r[\Lambda_i^2 - (E_\alpha - E_{\alpha'})^2]]\}, \end{aligned} \tag{6}$$

where Λ_i is a cut-off momentum and m_i is the mass of meson i, while E_α denotes the relativistic total energy of a nucleon in state α.

3. – Hartree approximation.

3·1. *Relativistic form.* – The Hartree approximation for the single-particle potential can be derived from the model Hamiltonian (2) in the usual way [4, 5]. It is a local and energy-independent operator. In a doubly magic nucleus, the corresponding relativistic single-particle wave equation reads

$$\{\boldsymbol{\alpha}\cdot\boldsymbol{p} + \gamma_0[m + U^{\text{H}}_s(r) + \gamma_0 U^{\text{H}}_0(r)]\}\, \psi_q(\boldsymbol{r}) = E_q\, \psi_q(\boldsymbol{r}), \tag{7}$$

where the upper index H refers to « Hartree » and the lower index q labels the eigenstates. The scalar and the vector relativistic single-particle potentials are given by

$$U^{\text{H}}_s(r) = -\int d^3r'\, \varrho_s(r')\, V^{\alpha\alpha}_\sigma(|\boldsymbol{r} - \boldsymbol{r}'|), \tag{8}$$

$$U^{\text{H}}_0(r) = \int d^3r'\, \varrho(r')\, V^{\alpha\alpha}_\omega(|\boldsymbol{r} - \boldsymbol{r}'|). \tag{9}$$

Here $\varrho(r)$ and $\varrho_s(r)$ are the baryon density and the self-consistent scalar density, respectively,

$$\varrho(r) = \sum_{q=1}^{A} \psi^\dagger_q(\boldsymbol{r})\, \psi_q(\boldsymbol{r}), \tag{10}$$

$$\varrho_s(r) = \sum_{q=1}^{A} \bar{\psi}_q(\boldsymbol{r})\, \psi_q(\boldsymbol{r}). \tag{11}$$

The sums in eqs. (10) and (11) run over the A lowest occupied eigenstates.

These relations take a simple form in the case of nuclear matter. If k_{F} denotes the Fermi momentum, one then finds [7]

$$U^{\text{H}}_0 = \frac{g_\omega^2}{m_\omega^2}\, \varrho, \qquad U^{\text{H}}_s = -\frac{g_\sigma^2}{m_\sigma^2}\, \varrho_s, \tag{12}$$

$$\varrho = \frac{2}{3\pi^2} k_{\text{F}}^3, \qquad \varrho_s = \frac{4}{(2\pi)^3} \int_0^{k_{\text{F}}} d^3k \frac{m^*}{[k^2 + m^{*2}]^{\frac{1}{2}}}, \tag{13}$$

where

$$m^* = m + U^{\text{H}}_s \tag{14}$$

is the « effective mass ». In the Hartree approximation, the average binding energy per nucleon is given by

(15) $$\frac{B}{A} = \sum_{k<k_F} \left[T(k) + \frac{1}{2} \Sigma(k) \right],$$

where

(16) $$T(k) = \langle \psi_k | \gamma_0 (\boldsymbol{\gamma} \cdot \boldsymbol{k} + m) | \psi_k \rangle - m$$

and

(17) $$\Sigma(k) = \langle \psi_k | U_0^H + \gamma_0 U_s^H | \psi_k \rangle$$

denote the relativistic kinetic energy and the potential energy, respectively, of a nucleon with momentum $\boldsymbol{k}$.

The results presented below have been obtained from the following parameter values

(18a) $$g_\sigma^2/4\pi = 6.57\,, \qquad m_\sigma = 550 \text{ MeV}\,,$$

(18b) $$g_\omega^2/4\pi = 9.25\,, \qquad m_\omega = 782.8 \text{ MeV}\,,$$

and with a cut-off form factor characterized by a mass $\Lambda = 1530$ MeV. These are the values which had been adopted by BROCKMANN [5] in his self-consistent relativistic Hartree calculation of the ground states of ^{16}O and of ^{40}Ca. They are identical to the σ- and ω-meson parameters of the one-boson exchange potential (OBEP) of the Bonn group [10]. We emphasize, however, that the latter property does not imply that this particular choice has any « fundamental » implication. Indeed, the Bonn OBEP contains a number of components which are omitted here and correspond to the exchange of other mesons (π, ρ, ...). Moreover, there certainly exist sizable corrections to the Hartree approximation, due to the Fock term (sect. 4) and to higher-order diagrams [8, 11]. In general, the input meson parameters of a Hartree or of a Hartree-Fock calculation should, therefore, be considered as *effective* coupling constants and masses [1]. We return to this point in sect. 5.

The full curve in fig. 1 represents the average binding energy per nucleon as calculated from the Hartree approximation (15). We note that at saturation the calculated Fermi momentum ($k_F = 1.51$ fm^{-1}) and the calculated average binding energy per nucleon ($B/A = -21.6$ MeV) are both larger than the empirical values ($k_F \simeq 1.36$ fm^{-1}, $B/A \simeq -16$ MeV). This indicates, in particular, that in finite nuclei the root-mean-square radius of the density distribution as calculated from this relativistic Hartree model will be somewhat too small. This is confirmed by Brockmann's calculation [5]. It can be checked that eqs. (12)-(17) are identical to those derived by WALECKA [1] in the framework of his « mean-field approximation ». They differ from the direct part of the lowest-order contribution to the self-energy [8] by the fact that here

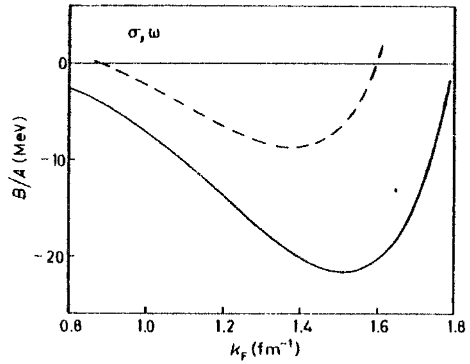

Fig. 1. – Dependence upon the Fermi momentum k_F of the average binding energy per nucleon as calculated from the input parameter (18). The full curve corresponds to the Hartree approximation and the dashed one to the Hartree-Fock approximation.

the effective mass m^* has to be calculated self-consistently from eqs. (12)-(14). Correspondingly, the spinor ψ_k in eq. (17) does not describe a free plane wave, but it instead includes the effect of the Hartree potential $U_s^H + \gamma_0 U_0^H$. It appears that this self-consistent requirement has been partly neglected in ref. [11]. We also note that the baryon density ϱ differs from the scalar density ϱ_s (see eqs. (13)). Figure 2 shows that this difference increases with increasing Fermi momentum. This has the effect of increasing the density at saturation as compared to the value that it would take if one would set $\varrho_s = \varrho$.

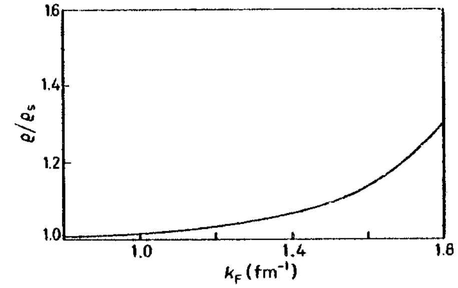

Fig. 2. – Ratio between the baryon density ϱ and the scalar density ϱ_s, as calculated from eqs. (13) with the input parameters (18).

3·2. *Nonrelativistic form.* – In the case of finite nuclei, one possible test of the relativistic Hartree approximation consists in comparing with experiment the bound single-particle energies E_k and the baryon density distribution $\varrho(r)$ calculated from the self-consistent set of eqs. (7)-(11) [4, 5]. However, one can perform a more severe test. Indeed, the accumulation of data on bound and, mainly, scattering states of many nuclei have led to a very good knowledge of the shell model potential. In its practical formulation, the latter is a local, energy-dependent operator which, when substituted in the nonrelativistic Schrödinger equation, yields the experimental single-particle energies and, if supplemented by an imaginary component, the experimental elastic-scattering phase shifts. Hence it is useful to construct here a potential which, when inserted in a Schrödinger equation, yields the same bound-state energies and the same elastic-scattering phase shifts as those which would be obtained from the relativistic Dirac equation (7). We dub this potential the « Schrödinger-equivalent potential » and we denote it by $U_e(r, \varepsilon)$, where $E = \varepsilon + m$. Its construction proceeds as follows.

Let us denote by $G(r;\varepsilon)$ the radial part of the large components of the relativistic single-particle wave function $\psi_a(r)$. It can easily be shown [5] that the quantity

$$g(r;\varepsilon) = [D(r;\varepsilon)]^{-\frac{1}{2}} G(r;\varepsilon) \tag{19}$$

with

$$D(r;\varepsilon) = \varepsilon + 2m + U_s^{\text{II}}(r) - U_0^{\text{II}}(r) \tag{20}$$

fulfils the following Schrödinger-like radial wave equation [7]

$$\frac{d^2 g(r;\varepsilon)}{dr^2} + \left\{k_\infty^2 - \frac{l(l+1)}{r^2} - 2m\left[U_e(r;\varepsilon) + \frac{1}{r}\, U_{so}(r;\varepsilon)\,\sigma\cdot L\right]\right\} g_k(r;\varepsilon) = 0\,, \tag{21}$$

where k_∞ denotes the relativistic momentum at large distance

$$k_\infty^2 = 2m\varepsilon + \varepsilon^2\,, \tag{22}$$

while

$$U_e(r;\varepsilon) \simeq U_s(r) + U_0(r) + (2m)^{-1}[U_s^2(r) - U_0^2(r)] + \frac{\varepsilon}{m}\, U_0(r)\,, \tag{23}$$

$$U_{so}(r;\varepsilon) = -[2mD(r;\varepsilon)]^{-1}\frac{d}{dr}[U_s(r) - U_0(r)]\,. \tag{24}$$

Here and in the following we usually drop the upper index II, for simplicity. In eq. (23), the sign $\simeq$ refers to the omission of negligible surface terms. We note that U_e depends on energy and that the Schrödinger-equivalent potential contains a spin-orbit component.

The quantities $U_e(r;\varepsilon)$ and $U_{so}(r;\varepsilon)$ can be compared with the central and spin-orbit components of the empirical shell model potential. The quantity which is best determined by the experimental data is the volume integral per nucleon

$$J_{U_e}/A = A^{-1}\int d^3r\, U_e(r;\varepsilon)\,. \tag{25}$$

Figure 3 shows that in the case of ^{40}Ca the calculated and empirical values of this quantity are in good agreement over a wide energy range. The same holds in the case of ^{16}O [6]. The calculated and empirical values of the spin-orbit component $U_{so}(r;\varepsilon)$ are also in fair agreement [7].

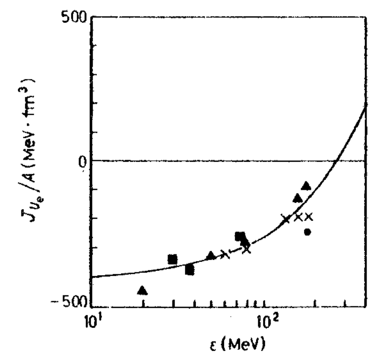

Fig. 3. – Adapted from ref. [7]. Comparison between the empirical (crosses, triangles, squares, dot) values of the volume integral per nucleon (25) and the theoretical (full curve) value calculated from the self-consistent Hartree approximation with the input parameters (18), in the case of ^{40}Ca.

We now turn to a brief discussion of the meaningfulness of these agreements. The model contains two main parameters, namely the strengths U_0 and U_s of the vector and of the scalar potentials at the Fermi momentum $k_F = 1.35\ \text{fm}^{-1}$, which corresponds to the central density of nuclei. The theoretical potential depth U_e is energy dependent, with a slope given by U_0/m (see eq. (26) below). Since the empirical value of this slope is approximately equal to 0.3, the value of U_0 must be approximately equal to 300 MeV. Since, moreover, the depth U_e at low energy is approximately equal to -55 MeV, one must have $U_s = -350$ MeV. This shows that the model parameters can always be chosen in such a way that U_e is in fair agreement with experiment at low and intermediate energies. Then, however, no parameter is left: U_{so} is uniquely predicted by the model; the fair agreement between the empirical and experimental values of $U_{so}(r;\varepsilon)$ is, therefore, by no means a trivial consequence of the choice of the input parameters.

Another noticeable and unavoidable feature of the present model is that U_0 and U_s are comparable in magnitude to the nucleon rest mass. Hence it appears that a relativistic approach is not a luxury. Indeed, it is then quite difficult to derive a Schrödinger equation as an accurate nonrelativistic limit of the Dirac equation (7). In particular, the Foldy-Wouthuysen transformation is not very useful [7]. We emphasize that the Schrödinger-like equation (21) is exact in the sense that the eigenvalues calculated from eq. (21) are the same as those of eq. (7) and that the asymptotic behaviour of $g(r; \varepsilon)$ for large r is the same as that of $G(r; \varepsilon)$. In order to complete the proof that it is legitimate to identify $U_e(r; \varepsilon)$ with the standard nonrelativistic optical-model potential, one must still show that the differential elastic-scattering and polarization cross-sections can be obtained in the same way from eq. (21) as from the usual phase-shift formula associated with the Schrödinger equation. This can be checked by comparing the equations contained in ref. [12, 13].

3'3. *Wine bottle bottom shape.* – In infinite nuclear matter, the Schrödinger-equivalent potential reads

$$U_e(\varepsilon) = U_s + U_0 + (2m)^{-1}[U_s^2 - U_0^2] + \frac{\varepsilon}{m} U_0, \tag{26}$$

where U_0 and U_s are given by eqs. (12) in the case of the Hartree approximation. This quantity is plotted in fig. 4 for two values of the Fermi momentum, namely $k_F = 1.35\ \text{fm}^{-1}$, which corresponds to the nuclear interior, and $k_F = 1.10\ \text{fm}^{-1}$, which corresponds to the nuclear surface. We note that the two curves intersect. This indicates that in a finite nucleus the Schrödinger-equivalent potential is still attractive at the nuclear surface at the energy at which it becomes repulsive in the nuclear interior. This « wine bottle bottom shape » is exhibited in fig. 5. Its origin has been discussed in ref. [6, 7]. It mainly lies in the quadratic term $(2m)^{-1}[U_s^2 - U_0^2]$ in eq. (23). This quadratic term is characteristic of the relativistic Dirac approach and of the scalar and

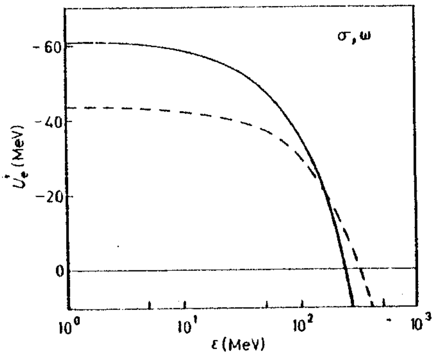

Fig. 4. – Schrödinger-equivalent potential in the case of infinite nuclear matter with $k_F = 1.35\ \text{fm}^{-1}$ (full curve) and $k_F = 1.10\ \text{fm}^{-1}$ (dashed curve), in the case of the relativistic Hartree approximation with the input parameters (18).

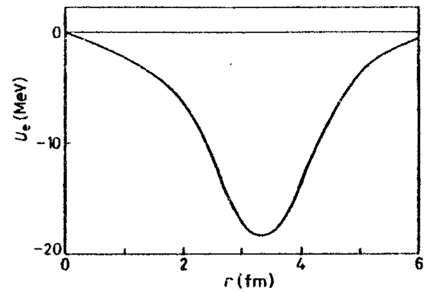

Fig. 5. – Adapted from ref. [7]. Schrödinger-equivalent potential as calculated from the relativistic Hartree approximation in the case of ^{40}Ca at $\varepsilon = 163$ MeV.

vector nature of U_s and of $\gamma_0 U_0$, respectively. Early empirical evidence for a wine bottle bottom shape was claimed by ELTON [14], who fitted polarization, reaction and elastic-scattering data for 180 MeV protons on ^{56}Fe. In fig. 6 we show that Elton's phenomenological potential is in fair agreement with the Schrödinger-equivalent potential as calculated from our nuclear-matter results by means of a local density approximation. Recent analyses of the scattering of 181 MeV protons by ^{40}Ca [15] and of 200 MeV protons by ^{12}C and ^{13}C [16] corroborate the existence of a wine bottle bottom shape for the real part of the optical-model potential. We note that this shape has also been found in a theoretical calculation performed in the framework of the Brueckner-Hartree-Fock approximation based on Reid's hard-core nucleon-nucleon interaction [17]. However, the interpretation of the phenomenon appears to be quite different in the latter theoretical model, in which it is due to Pauli and binding corrections [18].

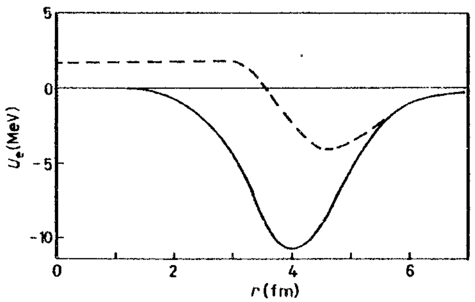

Fig. 6. – Adapted from ref. [7]. The dashed curve represents the real part of the optical-model potential determined by ELTON [14] from the analysis of 180 MeV protons scattering by ^{56}Fe. The full curve shows the Schrödinger-equivalent potential as calculated from the relativistic Hartree approximation with the input parameter (18) at 185 MeV.

4. – Hartree-Fock approximation.

4·1. *Schrödinger-equivalent potential in nuclear matter.* – In the relativistic Hartree-Fock approximation, the single-particle potential contains nonlocal terms, as in the familiar nonrelativistic case. In other words, the left-hand side of the relativistic Dirac single-particle wave equation (7) now contains an additional term of the form

$$\gamma_0 \int d^3r'\, U^{NL}(\boldsymbol{r}, \boldsymbol{r}')\, \psi_a(\boldsymbol{r}'), \tag{27}$$

where the upper index NL refers to «nonlocal», and where U^{NL} in general contains several components which transform as Lorentz-scalar, -vector, -pseudoscalar, ... quantities, respectively, if several types of mesons are considered [19]. In order to keep the discussion simple, it is advantageous to consider the case of infinite nuclear matter. Then $U^{NL}(\boldsymbol{r}, \boldsymbol{r}')$ is a function of $\boldsymbol{r}-\boldsymbol{r}'$ only, while

$$\psi_k(\boldsymbol{r}) = u(\boldsymbol{k}) \exp[i\boldsymbol{k}\cdot\boldsymbol{r}], \tag{28}$$

where $u(\boldsymbol{k})$ is a four-component spinor. It is then appropriate to use the momentum representation. It can be shown [8] that one can write the Fourier transform of $U^{NL}(|\boldsymbol{r}-\boldsymbol{r}'|)$ in the form

$$U^{NL}(\boldsymbol{k}) = U_s^{NL}(k) + \gamma_0 U_0^{NL}(k) + \gamma_0 \boldsymbol{\alpha}\cdot\frac{\boldsymbol{k}}{k} U_v^{NL}(k), \tag{29}$$

where the quantities U_s^{NL}, U_0^{NL} and U_v^{NL} are scalar functions of k, rather than matrices.

The form (29) is, of course, also valid for the local part, or equivalently for the momentum-independent part, of the single-particle potential. We thus temporarily drop the upper index NL. The relativistic single-particle wave equation reads

$$\left\{\boldsymbol{\alpha}\cdot\boldsymbol{k} + \gamma_0\left[m + U_s(k) + \gamma_0 U_0(k) + \gamma_0\boldsymbol{\alpha}\cdot\frac{\boldsymbol{k}}{k} U_v(k)\right]\right\} u(\boldsymbol{k}) = E_k u(\boldsymbol{k}). \tag{30}$$

In order to obtain a Schrödinger-equivalent potential, we proceed as in subsect. 3·2. We thus eliminate the small components of $u(\boldsymbol{k})$ and obtain the following dispersion relation ($E_k = \varepsilon_k + m$):

$$\frac{k^2}{2m} + U_e(k, \varepsilon) = \varepsilon + \frac{\varepsilon^2}{2m} = k_\infty^2 \tag{31}$$

with

$$U_e(k, \varepsilon) = U_0(k) + U_s(k) + (2m)^{-1}[U_s^2(k) - U_0^2(k) + U_v^2(k)] + \frac{\varepsilon}{m} U_0(k) + \frac{k}{m} U_v(k), \tag{32}$$

where k and ε are related to one another by eq. (31). By comparing this result with eq. (26), we note that, since all quantities now depend on the momentum k, one can probably not infer accurate information on each of these various quantities from our knowledge of the energy dependence of the depth of the empirical optical-model potential. One must thus turn to dynamical models. In the next subsection, we briefly discuss the Hartree-Fock approximation in the case of the σ, ω model.

4·2. *Hartree-Fock approximation.* – We restrict the present discussion to the case of infinite nuclear matter and to the σ, ω model. We only state some results. A detailed discussion will be published elsewhere. In keeping with the general expressions given in subsect. 4·1, the Hartree-Fock approximation yields the following relativistic single-particle wave equation

$$\{\boldsymbol{\alpha}\cdot\boldsymbol{k} + \gamma_0[m + U_s^H + \gamma_0 U_0^H + U^F(\boldsymbol{k})]\}\, u(\boldsymbol{k}) = E_k u(\boldsymbol{k}) \tag{33}$$

with

$$U^F(\boldsymbol{k}) = U_s^F(k) + \gamma_0 U_0^F(k) + \gamma_0\boldsymbol{\alpha}\cdot\frac{\boldsymbol{k}}{k} U_v^F(k). \tag{34}$$

The quantities U_0^H and U_s^H are still given by eqs. (12). However, the expression of ϱ_s which was given by eq. (13) in the Hartree approximation is now modified by the fact that the spinor $u(\boldsymbol{k})$ contains the influence of $U^F(k)$: one has

$$\varrho_s = \frac{4}{(2\pi)^3}\int_0^{k_F} d^3k \frac{\overline{m}(k)}{[k_v^2 + \overline{m}^2(k)]^{\frac{1}{2}}}, \tag{35}$$

where the momentum-dependent «effective mass» $\overline{m}(k)$ reads

$$\overline{m}(k) = m + U_s^H + U_s^F(k), \tag{36}$$

while

$$k_v = k + U_v^F(k). \tag{37}$$

The expressions of $U_s^F(k)$, $U_0^F(k)$ and $U_v^F(k)$ will not be given here. They are similar to results given in ref. [8, 20] with, however, some complications due to the fact that here we calculate $u(k)$ self-consistently rather than taking a free plane-wave spinor. One striking difference with the Hartree approximation is that the σ and the ω mesons both contribute to all three terms $U_s^F(k)$, $U_0^F(k)$ and $U_v^F(k)$.

It turns out that the contribution of $U_v^F(k)$ to the expression (32) of the Schrödinger-equivalent potential is rather negligible. For low k, the attractive quantity $U_s^F(k)$ is equal to about 25 per cent of the Hartree component U_s^H of the scalar potential; it tends towards zero for large k. For low k, the repulsive quantity $U_0^F(k)$ is equal to approximately forty per cent of the Hartree contribution U_0^H to the fourth component of the vector potential. The Schrödinger-equivalent potential $U_e^{HF}(\varepsilon)$ (fig. 7) that corresponds to the relativistic

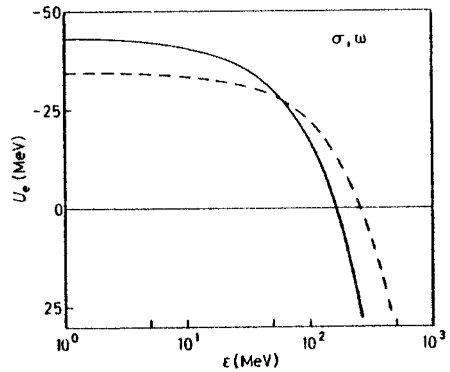

Fig. 7. – Schrödinger-equivalent potential in the case of infinite nuclear matter with $k_F = 1.35\ \text{fm}^{-1}$ (full curve) and $k_F = 1.10\ \text{fm}^{-1}$ (dashed curve), in the case of the relativistic Hartree-Fock approximation with the input parameters (18).

Hartree-Fock approximation in the σ, ω model is thus less attractive than the Schrödinger-equivalent potential associated with the relativistic Hartree approximation. Hence the fair agreement with the empirical shell model potential depth which had been found in the case of the relativistic Hartree approximation no longer holds for the Hartree-Fock approximation if one adopts the input parameters (18). Clearly, however, it is possible to somewhat increase the strength g_σ^2 of the coupling between the scalar and the nucleon fields in order to obtain a good agreement between the Hartree-Fock approximation and the empirical data. This increase would be legitimate, since we emphasized in subsect. 3·1 that the input parameters should be considered as « effective » coupling constants. We find it remarkable that the modification which is required is rather small. We also note that the two curves in fig. 7 intersect, as was also the case in fig. 4. This shows that the relativistic Hartree-Fock maintains a wine bottle bottom shape for the Schrödinger-equivalent potential at intermediate energy. In turn, this reflects the fact that the momentum dependence of $U_0^F(k)$ and of $U_s^F(k)$ is quite weak, because in the present model the effective nucleon-nucleon interaction has short range.

In the self-consistent relativistic Hartree-Fock approximation, the average binding energy per nucleon is given by

$$\text{(38)}\qquad \frac{B}{A} + m = \frac{3}{k_F^3}\int_0^{k_F} k^2\,\mathrm{d}k\left\{\frac{1}{2}\,U_0(k) + \frac{1}{2}\left[U_s(k)\,\overline{m}(k) + k_v U_v(k)\right]\cdot\left[k_v^2 + \overline{m}^2(k)\right]^{-\frac{1}{2}} + \left[m\overline{m}(k) + k_v k\right]\left[k_v^2 + \overline{m}^2(k)\right]^{-\frac{1}{2}}\right\}.$$

The quantity B/A as calculated from this approximation is represented by the dashed curve in fig. 1. As expected from the preceding discussion, it is less attractive than the Hartree-Fock approximation. Saturation is reached for $k_F = 1.36\ \text{fm}^{-1}$, where $B/A = -8.6$ MeV.

5. – Discussion.

The present contribution is centred on the belief that a formulation of the shell model in the framework of relativistic quantum field theory will lead to a relativistic Dirac single-particle wave equation rather than to a nonrelativistic Schrödinger single-particle wave equation. In the nonrelativistic approach, the shell model emerges from the Hartree-Fock approximation, in which the effective nucleon-nucleon interaction is in practice either adjusted in a purely phenomenological way or else is estimated from realistic nucleon-nucleon potentials via some (*e.g.* Brueckner) approximation scheme. Likewise, we considered here the shell model potential in the framework of a relativistic Hartree-Fock approximation. We adopted a simple model in which the interaction between two nucleons is mediated by the exchange of a scalar meson and of a vector meson [1]. To our knowledge, the present work is the first investigation in which the self-consistent Fock contribution is included. We focused on the prediction of this model concerning the average nucleon-nucleus potential, *i.e.* concerning the shell model potential or, more generally, the real part of the optical-model potential. For this purpose, we constructed a Schrödinger-equivalent potential. The latter is a single-particle potential which, when introduced in the nonrelativistic Schrödinger equation, yields the same bound-state energies and the same elastic-scattering phase shifts as the original relativistic single-particle potential did when used in conjunction with the Dirac equation. The comparison between this Schrödinger-equivalent potential and the central and spin-orbit components of the empirical optical-model potential is rather satisfactory, provided that the coupling constants between the nucleon and the meson fields are suitably adjusted. This adjustment corresponds to the use of an effective meson-nucleon interaction [1, 11]. One characteristic feature of the calculated Schrödinger-equivalent potential is that it has a « wine bottle bottom » shape at intermediate energy; in the present approach this shape is due to relativistic effects.

We hope that the relativistic Hartree-Fock model may become a workable and useful one if the experimental data are invoked to constrain the choice of the various meson-nucleon coupling constants. Here we have put emphasis on the single-particle potential at low and intermediate energy. Other data should, of course, be considered. The most stringent restrictions will probably arise from those observables which involve the small components of the relativistic single-particle spinors [21, 22]. We believe that a relativistic approach will become not only of theoretical but also of practical interest if it is eventually confirmed that the relativistic single-particle potential involves several components which are comparable in magnitude to the nucleon rest mass.

REFERENCES

[1] J. D. WALECKA: *Ann. Phys.* (*N. Y.*), **83**, 491 (1974).
[2] J. D. WALECKA: in *Nuclear Interactions*, edited by B. A. ROBSON (Berlin, 1978), p. 294, and references contained therein.
[3] B. D. SEROT and J. D. WALECKA: *Phys. Lett. B*, **87**, 172 (1979).
[4] L. D. MILLER and A. E. S. GREEN: *Phys. Rev. C*, **5**, 241 (1972).
[5] R. BROCKMANN: *Phys. Rev. C*, **18**, 1510 (1978).
[6] M. JAMINON, C. MAHAUX and P. ROCHUS: *Phys. Rev. Lett.*, **43**, 1097 (1979).
[7] M. JAMINON, C. MAHAUX and P. ROCHUS: *Phys. Rev. C*, **22**, 2027 (1980).
[8] S. A. CHIN: *Ann. Phys.* (*N. Y.*), **108**, 301 (1977).
[9] L. WILETS: in *Mesons in Nuclei*, edited by M. RHO and D. H. WILKINSON (Amsterdam, 1979), p. 789.
[10] K. ERKELENZ, K. HOLINDE and R. MACHLEIDT: unpublished. See also K. HOLINDE: Nordita preprint 79/16.
[11] M. R. ANASTASIO, L. S. CELENZA and C. M. SHAKIN: *Phys. Rev. C*, **23**, 569 (1981).
[12] N. F. MOTT and H. S. W. MASSEY: *The Theory of Atomic Collisions*, 3rd edition (Oxford, 1965), p. 228.
[13] A. INGEMARSSON: *Phys. Scr.*, **9**, 156 (1974).
[14] L. R. B. ELTON: *Nucl. Phys.*, **89**, 69 (1966).
[15] B. C. CLARK: private communication (1980).
[16] H. O. MEYER, P. SCHWANDT, G. L. MOAKE and P. P. SINGH: *Phys. Rev. C*, **23**, 616 (1981).
[17] J. P. JEUKENNE, A. LEJEUNE and C. MAHAUX: in *Nuclear Self-Consistent Fields*, edited by G. RIPKA and M. PORNEUF (Amsterdam, 1975), p. 155.
[18] C. MAHAUX: in *Common Problems in Low- and Medium-Energy Nuclear Physics*, edited by B. CASTEL (New York, N. Y., 1979), p. 265.
[19] L. D. MILLER: *Phys. Rev. C*, **9**, 537 (1974).
[20] M. BOLSTERLI: *Phys. Rev. D*, **11**, 312 (1975).
[21] J. V. NOBLE: *Phys. Rev. C*, **20**, 1188 (1979).
[22] J. M. EISENBERG: *Nucl. Phys. A*, **355**, 269 (1981).